CrystEngComm

Accepted Manuscript

ROYAL SOCIETY OF CHEMISTRY

www.rsc.org/crystengcomm

Journal Name

Cite this: DOI: 10.1039/c0xx00000x

www.rsc.org/xxxxxx

ARTICLE TYPE

Thermoelectric Metal Tellurides with Nanotubular Structures: Synthesized by Kirkendall Effect and their Reduced Thermal Conductivities

Zhanli Chai,[a] Hui Wang,[a] Quanyu Suo,[a] Niri Wu, [a] Xiaojing Wang,*[a] Cheng Wang*[b]

Received (in XXX, XXX) Xth XXXXXXXXX 20XX, Accepted Xth XXXXXXXXX 20XX
DOI: 10.1039/b000000x

ABSTRACT: Polycrystalline nanotubular Bi_2Te_3 and PbTe were synthesized through a high-temperature solution process using extracted metal-TOPO (trioctylphosphine oxide) precursors and Te nanowire as sacrificial template. X-ray diffraction, scanning electron microscope, transmission electron microscope, selected area electron diffraction, and high-resolution transmission electron microscope were employed to characterize the products. The formation of such tubular nanostructure is proposed to be the result of Kirkendall effect. Compared with single crystalline nanotube, such polycrystalline nanotubular structure is considered to have great influences on the thermal conductivity owing to the numerous grain boundaries. Transport properties of hot-pressed bulk samples formed by the as-prepared nanotubular products were investigated. Thermal conductivities of hot-pressed nanotubular samples were greatly reduced by around 80%, compared to the melting ones.

Introduction

High-efficiency thermoelectric (TE) energy conversion requires material with a large Figure of merit, $ZT = S^2\sigma T/\kappa$, in which S is the Seebeck coefficient, σ is the electric conductivity, κ is the thermal conductivity and T is the absolute temperature.[1-3] Many efforts have been pursued to enhance the thermoelectric ZT, including looking for advanced new families of TE materials with much higher power factor ($S^2\sigma$) and lower κ,[4-6] and reducing material's size to nanoscale.[1-3] The introduction of nanostructures will largely increase ZT values, which is attributed to the reduction of lattice thermal conductivity owing to increase phonon boundary scatterings,[7] and the enhancement of the power factor due to the quantum confinement effects.[8] Among the wide varieties of TE nanostructures, superlattice nanofilms, one-dimensional (1D) nanostructures, and quantum dots show remarkable enhancements in thermoelectric ZT.[9-12] For instance, ZT up to 2.5 was achieved for two-dimensional Sb_2Te_3/Bi_2Te_3 superlattice thin films, exceeding pervious limits of ~1 for the bulk counterpart,[9] and PbSeTe based quantum dots superlattice had higher ZT value as much as 1.7.[10] Even more exciting are the theoretical predictions for 1D nanostructures, which are given by calculations based on one-band mode and thought to have larger enhancement of ZT exceeding 5.[8, 11] This significant increase of ZT is attributed to the modified transport properties of 1D nanostructures, in which κ is decreased due to the phonon scattering at nanoscale interfaces, and σ is enhanced owing to the movement of electrons in a single dimension.[12-13] Compared with solid nanowires, 1D tubular structures will result in a further reduction in thermal conductivity because of the stronger phonon-surface scattering at inner and outer interfaces.[14]

TE metal tellurides, such as bismuth telluride (Bi_2Te_3), lead telluride (PbTe), antimony telluride (Sb_2Te_3) and so on, are traditional TE materials with better ZT in the state of the art.[9-10, 15] Among them, Bi2Te3 and its alloys have the highest ZT at room temperature and are now considered the best TE materials,[9] and PbTe with narrow bandgap (0.21 eV) is one of the most commonly used materials for solid-state TE devices that operate at medium temperatures (450-800 K).[10] Although many attempts have been made to prepare 1D nanostructures of these TE metal tellurides, such as electrodeposition,[16-17] physical vapor process,[18] solution-phase reactions,[19] molecular beam epitaxy,[20] and so on, most of these approaches have complex operations and low production yields, and limited works have been reported on the synthesis of their nanotubes.[21-26] For instance, X. G. Li's group found that highly crystalline Bi_2Te_3 nanotubes could be obtained through solution phase by Kirkendall effect,[26] and rectangular and single-crystal PbTe nanotubes were synthesized via a thermal chemical reaction process.[23] But so for, there is not a common route to prepare nanotubes for different TE metal tellurides, which is mainly due to the different crystal structures for diverse TE metal tellurides. Q_2Te_3 (Q = Bi, Sb) has rhombohedral unit cell that can be considered as groupings of -Te-Q-Te-Q-Te- planes,[15] however, PbTe is typical cubic rock-salt crystal structure.[27] Therefore, there are big differences in the selections of metal precursors and reaction approaches for different TE metal tellurides, which made it seem impossible to develop facile and effective route for their nanotubular structures.

Kirkendall effect, which refers to a nonreciprocal mutual diffusion process through an interface of two metals, has been widely applied in a nanoscale system and has attracted special attention for hollow nanostructures due to its generic feature.[28-30] There are two qualitative scenarios for the formation of good nanotubes by Kirkendall effect:[31] (i) a binary phase works better than a ternary one, and the outward diffusion of core material is much faster than the inward diffusion of the shell phase; (ii) the product phase should be rich of dislocations and grain boundaries (effectively polycrystalline), since these defects absorb vacancies that could exchange locations with the diffusion atoms. In addition, choosing the right reaction temperature is important and should assure sufficient diffusivities of the atoms and vacancies. In our previous report,[32] Kirkendall effect was successfully used to synthesize nanotubular Bi_2Te_3 structures. It was worth noting that the obtained Bi_2Te_3 product had polycrystalline structure and was a binary phase, moreover, the diffusion of Te core was faster than Bi shell mainly due to the much smaller atomic radius of Te. As we know, the relationships of atomic radius between Te and other common metals are as follows: tellurium (142 pm) < antimony (145 pm) < cadmium (148.9 pm) < bismuth (154.7 pm) < lead (175 pm). Thus, the diffusion of Te atom would be faster than these metal atoms, and in terms of theory, the binary metals formed by Te and Sb (or Cd, Bi, Pb) could have Kirkendall effect in solution phase. However, one of the big challenges is the selection of appropriate metal precursors in experiments. For the report of Bi_2Te_3 nanotube,[26] $BiCl_3$ dissolved in ethylene glycol (EG) solution was used as bismuth precursor, however, $PbCl_2$, which was insoluble in EG, couldn't be served as lead precursor for the formation of PbTe nanotube. In our previous high-temperature solution process,[32] nanotubular Bi_2Te_3 was prone to be synthesized in the conditions of low reaction temperature and weak reducing agent when Bi-TOPO was used as precursor, which was prepared through the extraction of bismuth ions by TOPO from $BiCl_3$ solution. In addition, other metals ions, such as Pb, Sb and so on, could also be extracted by TOPO from their soluble salts. Therefore, other nanotubular TE metal tellurides would be probably obtained by Kirkendall effect using these extracted metal precursors in similar high-temperature solution process.

In the typical synthesis, polycrystalline nanotubular Bi_2Te_3 and PbTe were prepared by high-temperature solution approach, which included two-step process: the synthesis of Te nanowires at high temperature and subsequent synthesis of polycrystalline nanotubular metal tellurides at low temperature. X-ray diffraction (XRD) patterns, scanning electron microscope (SEM), transmission electron microscope (TEM), selected area electron diffraction (SAED), and high-resolution TEM (HRTEM) were employed to characterize the products. The possible formation mechanism of the nanotubular structures was also discussed. Transport properties of hot pressed nanotubular samples, including S, σ, and κ, were finally investigated and compared with those of the melting samples.

Experimental

Chemicals. Trioctylphosphine oxide (TOPO, 90.0%) and oleylamine (70.0%) were purchased from Aldrich. Oleic acid (OA, AR), tributylphosphine (TBP), bismuth oxide (Bi_2O_3, AR), lead nitrate ($Pb(NO_3)_2$, AR), tellurium powder (>98.0%) and phenylhydrazine (PHZ, 98.0%) were purchased from Sinopharm Chemical Reagent Co., Ltd.

Preparation of the bismuth/lead precursor. 2.91 g Bi_2O_3 was dissolved in 10.0 ml 6.0 M HCl aqueous solution at 80 ^oC to form $BiCl_3$ aqueous solution. The formed $BiCl_3$ in above dissolution process (or 5.05 g lead nitrate) was dissolved in aqueous solution. Then, bismuth (or lead) ions were extracted from the aqueous solution by 8.40 g TOPO and formed metal-organic precursor based on bismuth (or lead) extracted in TOPO (abbreviated as Bi-TOPO, Pb-TOPO). The extraction yield was about 80.6% for bismuth (84.5% for lead) in this system.

Preparation of tellurium precursor. 1.38 g tellurium powder was dissolved in heated 10.0 ml 3.0 M HNO_3 aqueous solution. After dissolution, this solution was subjected to evaporation till dryness. The dried white powder was dissolved in 10.0 ml 6.0 M HCl aqueous solution, then 8.40 g TOPO was used to extract tellurium ions from this solution by keeping the whole extraction system in an oven at 60 ^oC. Te extraction yield in TOPO is about 95.2%.

Synthesis of tellurium nanowires. In a typical experiment, 2.0 ml oleylamine and 2.0 ml oleic acid (OA) were loaded in a 50.0 ml three-neck flask equipped with a condenser and then heated to 200 ^oC with flow nitrogen under constant stirring. 0.2 ml Te-TOPO stock solution was rapidly (< 1 s) injected into the solvents, and the reaction was kept at the same temperature for 10 min.

Preparation of nanotubular Bi_2Te_3 (PbTe). The temperature of the flask containing Te nanowires prepared in previous step was lowered to 80 ^oC, and then 0.3 ml Bi-TOPO (or Pb-TOPO) and 0.3 ml PHZ were simultaneously injected into the solution. After injection, the temperature would rise to about 86 ^oC and white smoke was released from the reaction system, probably due to the oxidations of PHZ or chlorine ions from the extracted species. The temperature would decrease to 80 ^oC within 5 min and the reaction was maintained in such system for 12 h. The obtained precipitate was washed by absolute ethanol and tributylphosphine (TBP) to remove organic solvents and excess tellurium, and then dried in oven for further characterization.

Structure Characterizations. XRD patterns were recorded with a Rigaku-Dmax2500 diffractometer using Cu K_α radiation (40 kV, 40 mA) at a step width of $8^o \cdot min^{-1}$. Field emission SEM images were taken using a JSM-6700F operated at an acceleration voltage of 10 kV. TEM images and SAED patterns were investigated on a JEOL-JEM-2010 operated at 200 kV. HRTEM images were tested on FEI Tecnai G2 F20 S-TWIN operated at 200 kV.

Thermoelectric transport characterization. We measured S, σ, and κ of samples composed of randomly aligned polycrystalline nanotubular Bi_2Te_3 (or PbTe) prepared by typical synthetic process. The as-prepared powders were heated to 500 ^oC in tube furnace with establishing a flow of oxygen, and then hot pressed into a rectangle pellet (1.5 cm in side length and 0.25 cm in thickness) using a pressure of 100 MPa at 150 ^oC for 10 min. Measurements were electronically controlled by an automatic measuring system (programmable current source Model 2400, multimeter Model 2000, switch system Model 7001, Keithley Instruments). For Seebeck measurements, a temperature gradient

was established between the substrate and the rectangle sample that was electrically heated. Four-point-probe method was adopted for the electric conductivity measurement. Thermal conductivities of as-obtained Bi_2Te_3 (or PbTe) pellets were determined by laser-flash technique on LFA 457 MicroFlash Netzsch apparatus, and were measured through thermal diffusivity (α) and specific heat (C_p) and then calculated via the equation $\kappa=\alpha\rho C_p$ (ρ is the density).

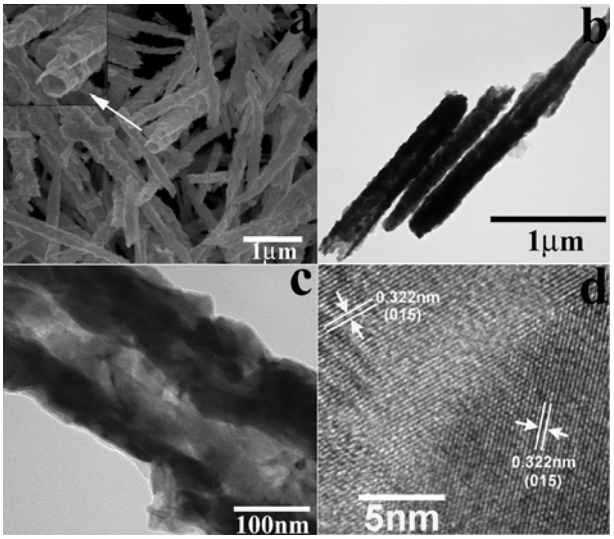

Fig. 1 FESEM image (a), TEM images (b and c), and HRTEM image (d) of as-obtained nanotubular Bi_2Te_3 in typical synthesis.

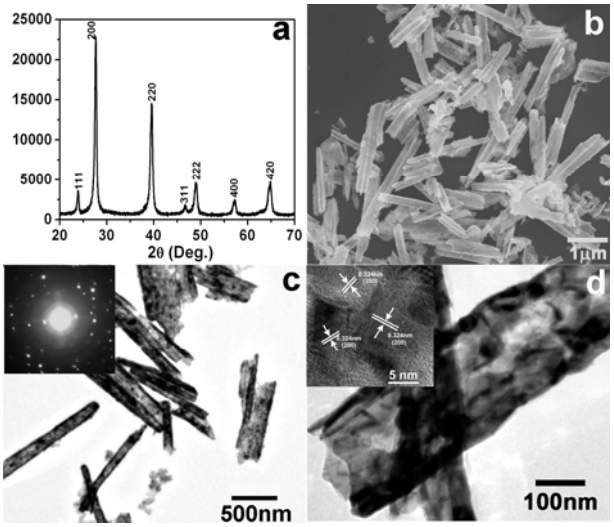

Fig. 2 The XRD pattern (a), FESEM image (b), TEM images (c and d), SAED pattern (inset of c) and HRTEM image (inset of d) of as-obtained PbTe nanotubes in typical synthesis.

Results and discussion

As reported in our previous research,[32] polycrystalline nanotubular Bi_2Te_3 with pure rhombohedral structure was obtained from the typical synthesis with Bi-TOPO as precursor. The FESEM and TEM images in Fig. 1 indicate that the as-prepared Bi_2Te_3 with length of several micrometers and diameter of 200-300 nm exhibits nanotubular structure. Furthermore, the surface of the tubular structure looks roughly under both FESEM and TEM indicating random growth and polycrystalline nature of

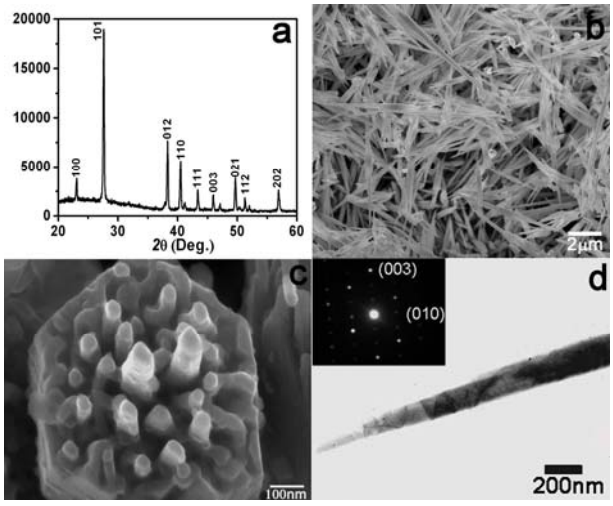

Fig. 3 The XRD pattern (a), FESEM images (b and c), TEM image (d) and SAED pattern (inset of d) of as-obtained Te nanowires in typical synthesis.

Bi_2Te_3. The hollow structure of the obtained Bi_2Te_3 could be seen from the high magnification SEM image shown in the inset of Fig. 1a and the TEM image shown in Fig. 1c. And the wall of nanotubular structure is 50-70 nm in thickness and formed by small pieces of nanosheets, which is revealed in Fig. 1c. As seen in the HRTEM image (Fig. 1d) taken from the edge of the nanotube in Fig. 1c, the measured distances of the neighboring lattice fringes are all 0.322 nm, corresponding well to the (015) lattice spacing for the rhombohedral Bi_2Te_3 phase.

When Pb-TOPO was used as precursor in typical synthetic process, the products were readily index to pure face-centered-cubic (fcc) PbTe with a space group $Fm\bar{3}m$ (JCPDS: 78-1905), which could be seen from the XRD pattern in Fig. 2a. As shown in Fig. 2b, the obtained PbTe products are mostly (>95%) rod-like structures with diameter of 200-400 nm and length of up to several micrometers. And the PbTe products also show nanotubular structures with much more obvious hollow interior as seen in Fig. 2c-d, compared with the obtained Bi_2Te_3. In addition, the thickness of the wall for PbTe nanotube is around 20 nm as shown in Fig. 2d and the wall of PbTe nanotube is probably built by nanoparticles with diameters of several tens of nanometers as seen in the HRTEM image (the inset of Fig. 2d). Similar with the obtained Bi_2Te_3 structures, the SAED pattern (inset of Fig. 2c) taken on the edge of nanotube indicates the polycrystalline nature of as-prepared PbTe products. Meanwhile, the HRTEM image shows that the lattice fringes are structurally uniform with a spacing of 0.324 nm, which is in good agreement with the d value of the (200) planes of fcc PbTe.

In typical synthetic process, tellurium products were firstly synthesized, which probably had important influences on the formation of nanotubular Bi_2Te_3 and PbTe. Fig. 3 shows the XRD pattern, FESEM and TEM images, and SAED pattern of the tellurium products. All peaks in the XRD pattern (Fig. 3a) correspond to the reflections of trigonal phase tellurium (JCPDS 36-1452). As shown in Fig. 3b, the products contains a few amount of nanoparticles and tapered nanowires with diameter of around 200 nm and length of 3-5 μm. And several nanowires

grow from the cross-section of Te nanoparticle seed as seen from

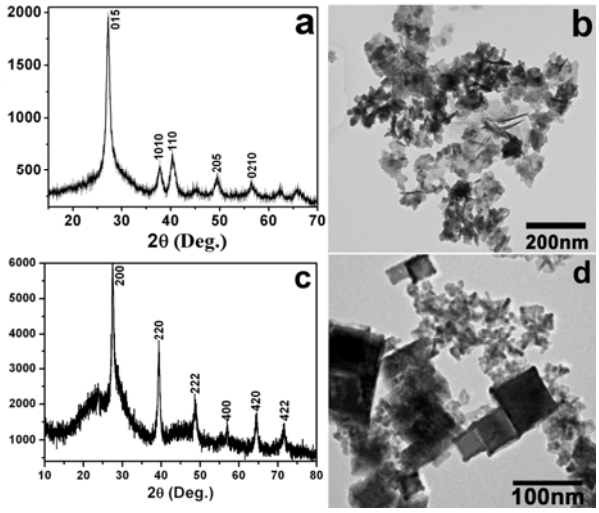

Fig. 4 The XRD pattern (a) and TEM image (b) of Bi_2Te_3, and XRD pattern (c) and TEM image (d) of PbTe obtained by simultaneously injecting two metal precursors (Bi-TOPO or Pb-TOPO and Te-TOPO) and PHZ into the reaction solution at 80 ^oC for 12h.

Fig. 3c, moreover, the nanowires grown from the center are much wider and longer than that from the edges. As reported in the literature,[33] tellurium nanotubes could be produced from Te particle seeds due to the much faster growth rate of Te nanowires from the edge than the center of Te seed. For our obtained Te products, the growth rate of Te particle seed from the center is much faster than that from the edge, which is probably the main reason for the formation of tapered Te nanowires. The TEM image in Fig. 3d exhibits the tapered Te nanowires with smooth surfaces. And the SAED pattern (inset of Fig. 3d) taken on the end of tapered nanowire shows good crystallinity of Te nanowires.

In literature works, TOPO, oleylamine and oleic acid were commonly used high-temperature solvents and surfactants. However, Bi_2Te_3 nanoplatelets[34] and PbTe nanocrystals or nanocubes[35] showed majority products when the two metal precursors were added simultaneously. Herein, two groups of comparative experiments were prepared. One was that metal precursors (Bi-TOPO and Te-TOPO) and reducing agent (PHZ) were simultaneously injected into the solvents at 80 ^oC and the mixture was maintained for 12 h. As shown in Fig. 4a, pure rhombohedral Bi_2Te_3 was also obtained, however, the grain size of the product is about 12 nm as calculated from Sherrer equation. The exact particle morphology, as seen from TEM result in Fig. 4b, contains small nanosheets with less than 100 nm in size and Bi_2Te_3 nanoparticles (10-20 nm in diameter) with some degree of agglomeration. When Bi-TOPO was replaced by Pb-TOPO, pure fcc PbTe is indexed from the XRD pattern in Fig. 4c and the grain size of as-prepared PbTe is around 25 nm as calculated from Sherrer equation. As shown in TEM image (Fig. 4d), several nanocubes with different diameters from 30 nm to 120 nm were obtained and accompanied by some nanoparticles with diameter of 10-20 nm and some degree of agglomeration. Therefore, the nanotubular structures of Bi_2Te_3 and PbTe all couldn't be produced unless the prior formation of tellurium nanowires.

Although Te nanowires could be seen as template for nanotubular metal tellurides, the formation process of these

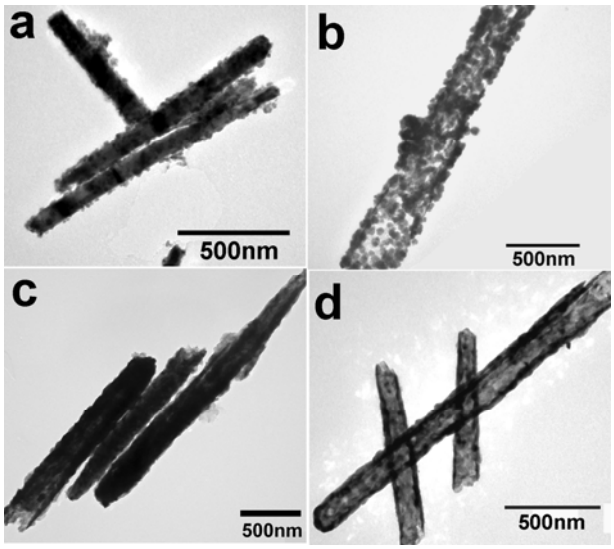

Fig. 5 TEM images of PbTe products formed in typical synthetic process with (a) reaction duration of 30 min, (b) reaction duration of 30 min and remove of Te by TBP, (c) reaction duration of 12 h, and (d) reaction duration of 12 h and remove of Te by TBP.

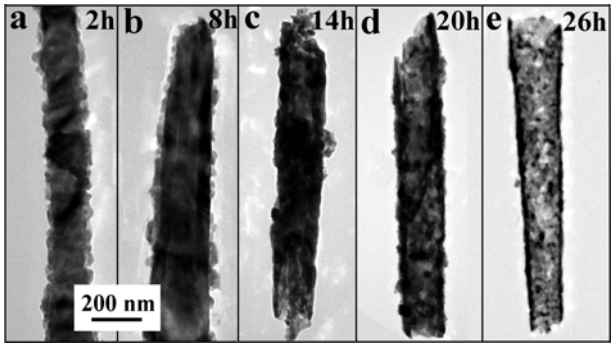

Fig. 6 TEM images of PbTe products formed in typical synthetic process with reaction duration of (a) 2 h, (b) 8 h, (c) 14 h, (d) 20 h, (e) 26 h.

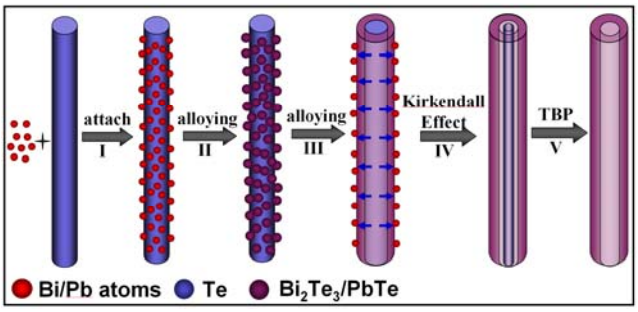

Fig. 7 Schematically illustrated shape evolution process from Te solid nanowire to Bi_2Te_3 (or PbTe))nanotube.

nanotubular structures is still unknown. Fig. 5 and Fig. 6 shows PbTe products obtained in typical synthetic process with different reaction durations. When Pb-TOPO precursor reacted with Te nanowires and PHZ for 30 min, nanowires with rough surface formed by the adhesion of nanoparticles could be seen from Fig. 5a. After the remove of tellurium by TBP, nanotubular structure with rough surface formed by single layer of nanoparticles is shown in Fig. 5b. The results of Fig. 5a-b indicate that PbTe

nanoparticles are firstly produced on the surface of Te nanowires. When the reaction duration was increased to 12 h, nanowires with much smoother surfaces and much thicker walls were prepared as shown in Fig. 5c, and obvious nanotubes could be seen in Fig. 5d after the products in Fig. 5c was post-disposed by TBP. The morphologies of the time-dependent PbTe products were carefully observed, as shown in Fig. 6. With the increase of reaction duration from 2 h to 26 h, the surfaces of nanowires became much smoother and hollow inners were much more obvious. The results in Fig. 5d and Fig. 6d-e reveal that PbTe products synthesized in much longer duration could also grow into nanotubes without the post-disposion by TBP. Thus, the alloying process between Pb and Te is indicated to be dependent on time the alloying rate is very slow due to the residual Te after 12 h.

Based on the time-dependent morphologies of PbTe nanotubes shown in Fig. 5 and Fig. 6, the shape evolution process from Te solid nanowire to Bi_2Te_3 (or PbTe) nanotube was schematically illustrated in Fig. 7. Firstly, the Bi (or Pb) atoms produced from Bi-TOPO (or Pb-TOPO) selectively nucleate at the side surfaces of Te nanowires (Step I in Fig. 7), and an alloying process is initiated to form Bi_2Te_3 (or PbTe) nanoparticles on the surface of Te nanowires (Fig. 6a and Step II in Fig. 7). Secondly, core-shell nanowires formed by Bi-Te alloy (of Pb-Te alloy) layer and core Te nanowires are subsequently obtained in further alloying process (Fig. 6b and Step III in Fig. 7). Although the diffusions of Bi (or Pb) and Te atoms through the Bi-Te (or Pb-Te) alloy layer are reciprocal, the diffusion rate of Te atom is much faster than

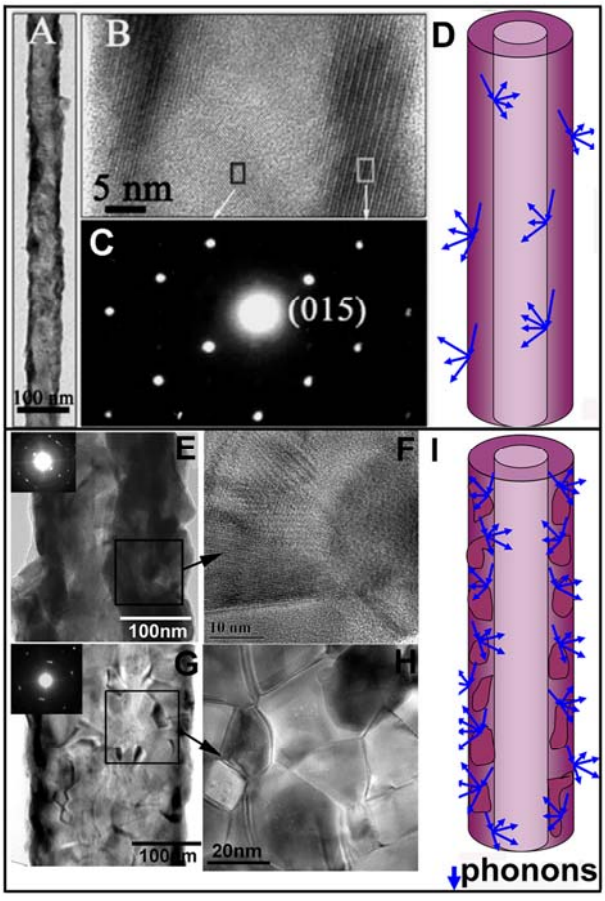

Fig. 8 The comparative morphologies and illustrations of phonon scatterings between single crystalline Bi_2Te_3 nanotube (A-D) in the literature[26] and as-synthesized polycrystalline Bi_2Te_3 and PbTe nanotubes (E-I) in typical synthesis.

Bi (or Pb) atom due to the much smaller atomic radius of Te than Bi or Pb. So it could be regarded as the nonreciprocal diffusion of Te core through the Bi-Te (or Pb-Te) alloy layer, which leads to void formation between the Bi-Te (or Pb-Te) alloy layer and the core Te nanowires, as shown in Figure 6c and the Step IV in Fig. 7. Finally, the unreacted Te nanowires are washed away by TBP and Bi_2Te_3 (or PbTe) nanotubular structures could be seen, which is indicated in Fig. 5d and the Step V in Fig.7. The observed shape evolution in Fig. 6 and illustrated shape evolution scheme in Fig. 7 provide strong evidences that the nanoscale Kirkendall effect is conducive to as-prepared TE metal tellurides (e. g. Bi_2Te_3 and PbTe) nanotubes.

As we know, the electrons for 1D nanostructures are confined to move in a single dimension long their axes, which could effectively improve σ. Apparently, single crystalline 1D nanostructures exhibit much higher σ than polycrystalline ones since the transport of electrons in single crystalline nanostructures is much more fluent due to the much less grain boundaries. However, owing to the increase of phonon boundaries, κ for polycrystalline 1D nanostructures is much lower than single crystalline ones. The comparative morphologies of single crystalline Bi_2Te_3 nanotube (A, B, C) in the literature[26] and as-synthesized polycrystalline Bi_2Te_3 (E and F) and PbTe (G and H) nanotubes were shown in Fig. 8. As seen from Fig. 8B and 8C, Bi_2Te_3 nanotube in the literature[25] showed obvious single crystalline nature. However, the as-obtained nanotubular Bi_2Te_3 and PbTe reveal polycrystalline structures from both the HRTEM images and SAED patterns as shown in Fig. 8E-H. In the high magnification TEM image (Fig. 8F) taken on the marked region of Bi_2Te_3 nanotubular structure in Fig. 8E, the wall of Bi_2Te_3 nanotubular structure is assembled by several Bi_2Te_3 small nanosheets, which would be the main reason for the formation of polycrystalline structure. Meanwhile, as shown in Fig. 8H, the high magnification TEM image taken on the marked region of PbTe nanotube (Fig. 8G) indicates that the wall of PbTe nanotube is adhered by many PbTe nanoparticles, which contributes to the polycrystalline PbTe structures. In addition, the illustrations of phonon scatterings in single crystalline and polycrystalline

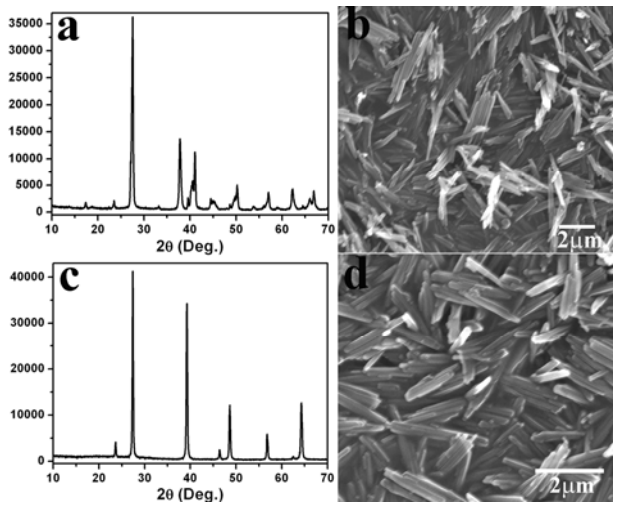

Fig. 9 The XRD pattern (a) and cross section SEM images (b) of hot-pressed nanotubular Bi_2Te_3 samples, and the XRD pattern (c) and cross section SEM images (d) of hot-pressed nanotubular and PbTe samples.

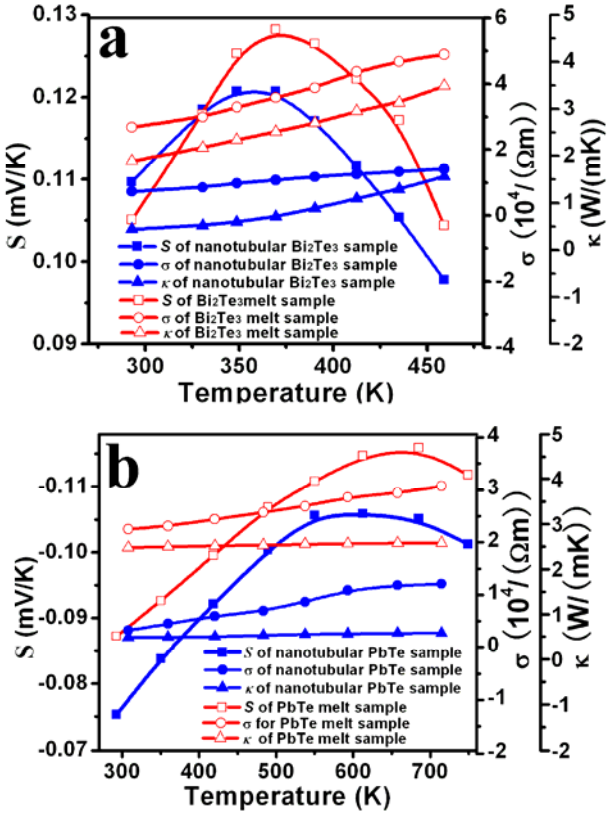

Fig. 10 S, σ and κ vs. substrate temperature of hot-pressed nanotubular Bi_2Te_3 (a, blue lines) and PbTe (b, blue lines) compared to their melt samples (red lines and open dots).

nanotube are demonstrated in Fig. 8D and 8I, respectively. For single crystalline 1D nanotube (Fig. 8D), the phonon boundaries are formed by the inner and outer surfaces of nanotubes, however, the amount of phonon boundaries for polycrystalline 1D nanotube will increase dramatically due to the numerous grain boundaries, as shown in Fig. 8I. Thus, the thermal conductivity of the as-synthesized TE metal tellurides with polycrystalline nanotubular structures would decrease compared with the single crystalline ones.

In our previous report,[32] the electric conductivity of obtained polycrystalline nanotubular Bi_2Te_3 was three orders of magnitude less than bulk bismuth telluride materials, which was mainly due to the much larger resistance brought by the insufficient contact between the nanotubular structures and resided organic agents on the surfaces of samples. Accordingly, the as-prepared Bi_2Te_3 or PbTe powders in this paper were heated at 500 °C in tube furnace with establishing a flow of oxygen for the remove of organic compounds on the surface; meanwhile, the as-obtained powders were hot pressed (150 °C) using a much higher pressure of 10 MPa in order to increase the relative density and decrease the resistance. The XRD patterns of the hot-pressed nanotubular Bi_2Te_3 and PbTe samples were shown in Fig. 9a and 9c, which showed that hot pressed Bi_2Te_3 and PbTe products had same structures but much bigger grain sizes compared with their samples before heat treatments. In Fig. 9b and 9d, the cross section SEM images of the hot-pressed nanotubular Bi_2Te_3 and PbTe samples reveal that 1D nanostructures and nanoscale grain boundaries have been well-preserved.

In order to indicate the transport properties of hot-pressed nanotubular samples, the melting samples were prepared for comparasion, which were obtained by the calcinations of as-prepared Bi_2Te_3 or PbTe powders at 800°C for 5h. The influences of substrate temperature on S, σ and κ were plotted in Fig. 10a for Bi_2Te_3 samples and Fig. 10b for PbTe samples, in which hot-pressed nanotubular samples were drawn in blue lines and melting samples were drawn in red lines. The positive sign of S in Fig. 10a indicates a p-type semiconductor behavior of the undoped Bi_2Te_3, and the pure PbTe is a n-type semiconductor according to the negative sign of S in Fig. 10b. The values of S increase firstly and then decrease with the elevation of temperature for both as-obtained Bi_2Te_3 and PbTe samples. In addition, the curves of σ elevate as the increase of temperature for both Bi_2Te_3 and PbTe. The influences of temperature on S and σ are essentially due to their dependence on carrier density, which can be written in following formula:

$$S = \frac{k}{e}\left\{\ln\left[\frac{N_c(t)}{n}\right] + m\right\}$$

$$\sigma = ne\mu$$

where k, e, $N_c(t)$, n, m, μ are, respectively, the Boltzmann constant, the elementary charge, the density of states for the conduction band, the carrier density, a constant and electron's mobility. When temperature is less than 350 K for Bi_2Te_3 (or 600 K for PbTe), carriers are mainly the holes in the valence band for p-type Bi_2Te_3 and the electrons in the conduction band for n-type PbTe, and the number of these carriers is almost independent on temperature. However, the density of states for the conduction band of intrinsic semiconductor will be increased with the elevation of temperature. Therefore, the curves of S elevate in temperature below 350 K for Bi_2Te_3 (or 600 K for PbTe). But when temperature is higher than 350 K for Bi_2Te_3 (or 600 K for PbTe), intrinsic excitation is dominant for this pure Bi_2Te_3 (or PbTe) material, so the value of S is reduced with the increase of carrier density when temperature is elevated. In addition, due to the increase of electron's mobility with the elevation of temperature owing to the better crystallization for hot-pressed bulk samples, the electric conductivities show obvious dependence on temperature for both Bi_2Te_3 and PbTe in Fig. 10a and 10b. Furthermore, the obtained electric conductivities (10^4 $\Omega^{-1}\cdot m^{-1}$) are approximately two orders of magnitude more than our previous report[32] mainly ascribed to the much lower resistance brought by removing organic matters and hot pressing. However, the values of σ are still apparently less than that of their melting samples, which is probably due to electron scatterings at numerous grain boundaries of polycrystalline nanostructures. As seen from κ curves in Fig. 10a and 10b, the thermal conductivities also increase with the elevation of temperature, which results from the weaker phonon scatterings at less grain boundaries with higher temperature. Furthermore, the lowest value of κ for hot-pressed nanotubular Bi_2Te_3 is 0.435 $W\cdot m^{-1}\cdot K^{-1}$, a reduction of 77% compared to that of Bi_2Te_3 melting sample. And the average reduction of κ for hot-pressed nanotubular PbTe

is up to 80%, compared to their melting samples. These significant decreases of κ indicate that nanotubular morphologies and polycrystalline natures of as-prepared Bi_2Te_3 and PbTe have significant effects on phonon transport.

Conclusions

Polycrystalline nanotubular Bi_2Te_3 and PbTe were prepared by high-temperature solution approach and had similar morphologies in length and diameter, however, they still had obvious differences in the thickness and formed nanostructures of the wall for nanotubes. The firstly synthesized Te nanowires in typical synthesis were used as sacrificial template, without which nanotubular Bi_2Te_3 or PbTe structures couldn't be produced. In the formation process, Kirkendall effect is conducive to as-prepared TE metal tellurides (such as Bi_2Te_3 and PbTe) with nanotubular structures. In addition, the numerous grain boundaries of polycrystalline nanotubular structure have great influences on the thermal conductivity of phonons. In the studies of transport properties, the values of σ for hot-pressed nanotubular samples are much lower than that of their melting samples, which could be attributed to the impediment of grain boundary to electron mobility. Meanwhile, the values of κ for hot-pressed nanotubular samples are reduced by nearly 80%, compared to their melting samples, which is ascribed to the strong phonon scatterings on grain boundaries of polycrystalline nanostructures. If the decrease of κ is much more than the reduction of σ, ZT of these polycrystalline nanotubular TE metal tellurides will be expected to be improved. Meanwhile, the selection of extracted TE metal precursors and the introduction of Kirkendall effect in high-temperature solution phase offer us a simple and large-scale production for different metal tellurides with nanotubular structures.

Acknowledgements

This work was supported by National Natural Science Foundation of China (Grant No. 21306075) and Inner Mongoia Natural Science Foundation of China (Grant No. 2011BS0201).

Notes and references

[a] Chemistry and Chemical Engineering Department, Inner Mongolia University, Inner Mongolia 010021 P. R. China. E-mail: *wang_xiao_jing@hotmail.com*

[b] State Key Laboratory of Rare Earth Resource Utilization, Changchun Institute of Applied Chemistry, Chinese Academy of Sciences, Changchun 130022, P.R. China. E-mail: *cwang@ciac.jl.cn*

1. A. I. Hochbaum, P. Yang, *Chem. Rev.*, 2010, **110**, 527.
2. Y. Zhao, J. S. Dyck, C. Burda, *J. Mater. Chem.*, 2011, **21**, 17049.
3. R. J. Mehta, Y. Zhang, C. Karthik, B. Singh, R. W. Siegel, T. Borca-Tasciuc, G. Ramanath, *Nat. Mater.*, 2012, **11**, 233.
4. J. R. Sootsman, D. Y. Chung, M. G. Kanatzidis, *Angew. Chem. Int. Ed.* 2009, **48**, 8616.
5. Y. Sun, P. Sheng, C. Di, F. Jiao, W. Xu, D. Qiu, D. Zhu, *Adv. Mater.*, 2012, **24**, 932.
6. S. K. Bux, A. Zevalkink, O. Janka, D. Uhl, S. Kauzlarich, J. G. Snyder and J. P. Fleurial, *J. Mater. Chem. A*, 2014, **2**, 215.
7. A. I. Hochbaum, R. Chen, R. D. Delgado, W. Liang, E. C. Garnett, M. Najarian, A. Majumdar, P. Yang, *Nature*, 2008, **451**, 163.
8. L. D. Hicks, M. S. Dresselhaus, *Phys. Rev. B*, 1993, **47**, 16631.
9. R. Venkatasubramanian, E. Siivola, T. Colpitts, B. O'Quinn, *Nature*, 2001, **413**, 597.
10. Harman, T. C.; Taylor, P. J.; Walsh, M. P.; LaForge, B. E. *Science*, 2002, **297**, 2229.
11. Y. M. Lin, M. S. Dresselhaus, *Phys. Rev. B*, 2003, **68**, 075304.
12. G. Zhang, Q. Yu, W. Wang, X. Li, *Adv. Mater.*, 2010, **22**, 1959.
13. Z. Li, Q. Sun, X. D. Yao, Z. H. Zhu and G. Q. Lu, *J. Mater. Chem.*, 2012, **22**, 22821.
14. R.Yang, G. Chen, M. S. Dresselhaus, *Nano Lett.*, 2005, **5**, 1111.
15. G. H. Dong, Y. J. Zhu and L. D. Chen, *CrystEngComm*, 2011,**13**, 6811.
16. H. Jung, D. Y. Park, F. Xiao, K. H. Lee, Y. H. Choa, B. Yoo, N. V. Myung *J. Phys. Chem. C*, 2011, **115**, 2993.
17. D. Chen, G. Chen, Q. Wang, R. Jin, Y. Wang, J. Pei, H. Xu and X. Shi, *CrystEngComm*, 2012, **14**, 7771.
18. Y. Deng, Y. Xiang, Y. Song, *Crys. Growth Des.*, 2009, **9**, 3079.
19. G. Zhang, H. Fang, H.Yang, L. A. Jauregui, Y. P. Chen, Y. Wu, *Nano Lett.*, 2012, **12**, 3627.
20. P. Dziawa, J. Sadowski, P. Dluzewski, E. Lusakowska, V. Domukhovski, B. Taliashvili, T. Wojciechowski, L. T. Baczewski, M. Bukala, M. Galicka, R. Buczko, P. Kacman, T. Story, *Cryst. Growth Des.*, 2009, **10**, 109.
21. Z. Wang, F. Q. Wang, H. Chen, L. Zhu, H. J. Yu, X. Y. Jian, *J. Alloys Comp.*, 2010, **492**, L50.
22. D. Pinisetty, M. Gupta, A. B. Karki, D. P. Young, R. V. Devireddy, *J. Mater. Chem.*, 2011, **21**, 4098.
23. J. Hu, Z. Chen, H. Jiang, Y. Sun, Y. Bando, D. Golberg, *J. Mater. Chem.*, 2009, **19**, 3063.
24. F. Xiao, B. Yoo, K. H. Lee, N. V. Myung, *J. Am. Chem. Soc.*, 2007, **129**, 10068.
25. X. Wang, Y. Xu, H. Zhu, R. Liu, H. Wang and Q. Li, *CrystEngComm*, 2011, **13**, 2955.
26. G. Zhang, Q.Yu, Z. Yao, X. Li, *Chem. Comm.*, 2009, 2317.
27. R. B. Soriano, I. U. Arachchige, C. D. Malliakas, J. Wu, M. G. Kanatzidis, *J. Am. Chem. Soc.*, 2013, **135**, 768.
28. H. J. Fan, M. Knez, R. Scholz, K. Nielsch, E. Pippel, D. Hesse, M. Zacharias, U. Gösele, *Nat. Mater.*, 2006, **5**, 627.
29. X. Liang, X. Wang, Y. Zhuang, B. Xu, S. Kuang, Y. Li, *J. Am. Chem. Soc.*, 2008, **130**, 2736.
30. M. H. Park, Y. H. Cho, K. Kim, J. Kim, M. Liu, J. Cho, *Angew. Chem. Int. Ed.*, 2011, **123**, 9821.
31. H. J. Fan, U. Gösele, M. Zacharias, *Small*, 2007, **3**, 1660.
32. Z. L. Chai, Z. P. Peng, C. Wang, H. J. Zhang, *Mater. Chem. Phys.*, 2009, **113**, 664.
33. B. Mayers, Y. Xia, *Adv. Mater.* 2002, **14**, 279.
34. J. S. Son, M. K. Choi, M. K. Han, K. Park, J. Y. Kim, S. J. Lim, M. Oh, Y. Kuk, C. Park, S. J. Kim, T. Hyeon *Nano Lett.*, 2012, **12**, 640.
35. J. J. Urban, D. V. Talapin, E. V. Shevchenko, C. B. Murray, *J. Am. Chem. Soc.*, 2006, **128**, 3248.

Thermoelectric Metal Tellurides with Nanotubular Structures: Synthesized by Kirkendall Effect and their Reduced Thermal Conductivities

Zhanli Chai,[a] Hui Wang,[a] Quanyu Suo,[a] Niri Wu,[a] Xiaojing Wang,[a] Cheng Wang*[b]*

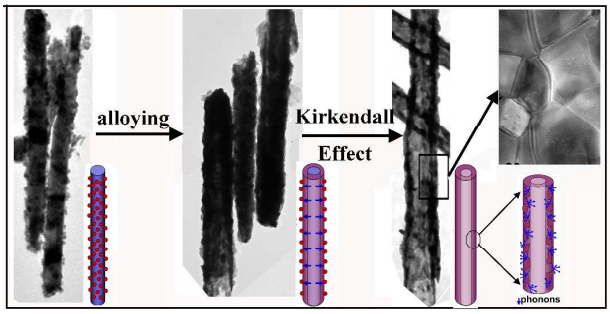

Polycrystalline nanotubular Bi_2Te_3 and PbTe synthesized by Kirkendall Effect showed great decreases in thermal conductivities.